ELSEVIER

Biochimica et Biophysica Acta 1275 (1996) 213–220

BBA Biochimica et Biophysica Acta

Evidence for two forms of the $g = 4.1$ signal in the S_2 state of photosystem II. Two magnetically isolated manganese dimers

P.J. Smith [b], R.J. Pace [a,*]

[a] *Department of Chemistry, Faculty of Science, Canberra, ACT 0200, Australia*
[b] *Plant Science Cooperative Research Centre, Australian National University Canberra, ACT 0200, Australia*

Received 7 February 1995; accepted 22 January 1996

Abstract

Two forms of the $g = 4.1$ signal in photosystem II (PS II) were identified from X-band and Q-band ESR signal shape and temperature dependence studies. Using ethylene glycol cryoprotected PS II illuminated at 130K, a $g = 4.1$ signal was generated which exhibited a temperature dependence consistent with it arising from a ground state species. Using sucrose cryoprotected PS II illuminated at 200K (in the absence of monoalcohols), a $g = 4.1$ signal was cogenerated with the multiline signal. At temperatures above ~ 20K, a signal at $g \sim 6$ became evident in these samples. The temperature dependencies of the multiline, $g = 4.1$ and $g \sim 6$ signals were quantitatively consistent with them arising from the first 3 states (spin 1/2, 3/2, 5/2) respectively of a weakly antiferromagnetically coupled Mn III-IV dimer. The temperature dependence of the signals in these samples indicated that the $g = 4.1$ signal now arose from a centre displaying excited state behaviour. The two types of $g = 4.1$ signal were very similar in shape at X-band but showed significantly different line shapes at Q-band. It is suggested that they arise from separate, near axial, $S = 3/2$ centres in well-defined states. A model is proposed, based on the temperature dependencies, ESR line shapes and probable spin states, to suggest that the four Mn ions are arranged as two exchange coupled pairs and that each $g = 4.1$ signal arises from a separate manganese dimer. The ground state $g = 4.1$ signal then requires the involvement of at least one additional spin 1/2 species, coupling to each Mn of a homodimer (probably IV-IV oxidation state). The spin 1/2 centre may be an oxidised protein side chain, possibly acting as a bridging ligand between the two Mn ions. It is concluded that the Mn dimers are sufficiently spatially separated within the protein structure to exclude magnetic exchange between the dimers, but within range to allow rapid electron transfer.

Keywords: Photosystem II; EPR; Manganese; 4.1 signal

1. Introduction

The photosynthetic process of oxidation of water to molecular oxygen is catalysed by the manganese containing oxygen evolving complex (OEC) of photosystem (PS) II in higher plants and algae. The minimum number of Mn ions required for functional water oxidation is four per reaction centre [1]. The location of the Mn binding sites and their protein environment, as well as the structure and catalytic mechanism operating at the Mn centre are as yet unresolved (see reviews [2–4]).

Dioxygen is photogenerated by the OEC via a four-step cyclic process involving five intermediate states, the S_i states (i = 0–4) [5]. For each advance of S_i state, an oxidative equivalent is generated and stored within the Mn-protein catalytic centre. On reaching the S_4 state, O_2 is released and the OEC returns to the S_0 state. In extensively dark adapted PS II samples, a majority of the OEC centres populate the S_1 state. EXAFS and XAS studies have indicated that the most likely Mn oxidation level in the S_1 state of PS II is $(MnIII)_2(MnIV)_2$ [6–9]. Photogeneration of a single turnover event at low temperature produces the S_2 state in high yield. EXAFS and XAS indicate the Mn oxidation level shifts to $(MnIII)(MnIV)_3$ [8,9].

Abbreviations: PS II, photosystem II; OEC, oxygen evolving centre; EG-L, ethylene glycol cryoprotected PS II illuminated at 130K; SUC-H, sucrose cryoprotected PS II illuminated at 200K; MES, 2-(N-morpholino)-ethanesulfonic acid; EDTA, ethylene-diamine-tetra-acetic acid (disodium salt); ESR, electron spin resonance; EXAFS, extended X-ray absorbance fine structure; XAS, X-ray absorbance spectroscopy; ZFS, zero field splitting.

* Corresponding author. Fax: +61 6 2490760.

PII S0005-2728(96)00012-6

The S_2 state is paramagnetic and two types of ESR signals arising from the Mn cluster are generated under various conditions. First, there is a signal centred near $g = 2$, characterised by 18–22 hyperfine features covering a width of 150–200 mT, known as the multiline signal [10–12]. In addition, a signal centred near $g = 4$ may be seen, characterised as a broad, relatively featureless resonance showing little resolved hyperfine structure under normal conditions, known as the $g = 4.1$ signal. [13–16]. These signals may be generated individually or cogenerated, depending upon the buffer cryoprotectant and illumination conditions applied to the PS II sample [13,14,17].

Most ESR studies on the multiline signal have been performed on PS II samples containing alcohol and illuminated at 200K, as this maximises the generation of the multiline signal without cogeneration of the $g = 4.1$ signal [10,11,14,16–18]. The alcohol is present in the sample as a solvent for DCMU and quinone acceptors. ESR studies on model compounds indicate that the minimal structure able to give rise to a hyperfine signal like the multiline would be a mixed valence Mn dimer, antiferromagnetically coupled, with a net spin of $S = 1/2$ [10,11,19]. ESR studies at different microwave frequencies (X-, P-, and S-bands) [20–23] have been interpreted to require that such a dimer must be part of a tetranuclear Mn structure, due to the complexity and number of lines in the hyperfine pattern, especially at S-band [20,23]. However, recent theoretical work in this laboratory simulating the multiline signal at S, X- and Q-band frequencies suggests that an isolated dimer, with a suitably anisotropic ligand environment, can explain the multiline pattern [24]. Temperature dependence studies on the multiline signal show that it arises from a centre displaying strict ground state behaviour over a temperature range 1.2K to 35K [17,25,26].

The $g = 4.1$ signal is most commonly generated by illumination of ethylene glycol or glycerol containing PS II samples at 130 to 140K [13,15,22,27]. Temperature dependence studies have shown that this low temperature generated $g = 4.1$ species exhibits Curie behaviour over a temperature range 4.5 to 30K [21,27]. Consequently, the centre giving rise to this $g = 4.1$ species, which must have a minimum spin of $3/2$, is a ground state, generated by a single electron withdrawal from a state having diamagnetic behaviour [28]. The involvement of at least 3 spin centres would appear to be required [27].

ESR studies on the $g = 4.1$ signal generated in ammonia treated PS II samples oriented onto mylar strips [29,30] have shown that at least 16 Mn hyperfine lines may be resolved in this signal, indicating that a minimum of two Mn ions are involved. The $g = 4.1$ signal generated in ethylene glycol cryoprotected PS II illuminated at 130K converts to a multiline signal upon short annealing at 200K (at a reduced intensity compared to samples initially illuminated at 200K) [13,15,27]. This interconversion at 200K has been hypothesised to result from a structural rearrangement of a Mn tetramer, interconverting from the $S = 3/2$ or $S = 5/2$ [9,13,21,22,31] structure responsible for the ground state $g = 4.1$, to the $S = 1/2$ structure responsible for the resulting multiline signal [15,27,32].

200K illumination of PS II samples containing sucrose as a cryoprotectant and no alcohol cogenerates the multiline and $g = 4.1$ signals [14,17,33,34]. Temperature dependence studies on these signals show clearly that the $g = 4.1$ species is an excited state and are consistent with the multiline and $g = 4.1$ signals arising from the ground ($S = 1/2$) and first excited ($S = 3/2$) states, respectively, of a Mn dimer (total spin $7/2$) [17,34]. Furthermore, ESR studies on these samples oriented onto mylar strips measured at X-band and unoriented PS II samples measured at Q-band have shown Mn hyperfine to be present on the $g = 4.1$ signals observed, indicating that the centre giving rise to this excited state $g = 4.1$ must contain at least two Mn ions also [34].

The above results lead to the somewhat surprising suggestion that *two types of '4.1' signals may be formed, one a ground and the other an excited state species.* The latter in particular is strongly indicated to be a near axial spin $3/2$ state [34]. The ground state form generated at very low temperatures, behaves in many respects as an 'intermediate' electron transfer species between the S_1 and stable (multiline) S_2 states of the OEC, and indeed was first interpreted as such by Casey and Sauer [13]. The major experimental variables determining which form of the $g = 4.1$ signal is observed appear to be the nature of the cryoprotectant (polyalcohols or sucrose) and the illumination temperature. In this study, we have utilised two common protocols for preparing PS II samples and examined the influence of the various cryoprotectant and illumination regimes on the resulting S_2 state ESR signals. We find that indeed two types of '4.1' signal may be photogenerated, with qualitatively different temperature dependencies. While these signals are of similar (but not identical) appearance at X-band frequency, they are quite distinguishable at Q-band. In addition, we have identified a new signal, at $g \sim 6$, associated with the excited state $g = 4.1$ species. This signal shows highly non-Curie behaviour, which is quantitatively consistent with it arising from a near-axial spin $5/2$ state, the next state above the spin $3/2$ $g = 4.1$ state. The implication of these findings for the Mn organisation in the OEC is briefly discussed.

2. Materials and methods

All preparations were undertaken at $\sim 4°C$ under dim green light with freshly harvested, washed spinach grown hydroponically in a greenhouse. PS II samples were prepared by two different Triton X-100 solubilisation procedures:

(1) Similar to that of Bricker et al. [35] with modifications according to Pace et al. [17] and stored in 15 mM NaCl, 10 mM $MgCl_2$, 20 mM MES (pH 6.0) (NaOH) plus cryoprotectant (Bricker PS II), and

(2) Similar to the method of Berthold et al. [36] with modifications according to Beck et al. [37] and stored in 15 mM NaCl, 5 mM EDTA, 5 mM $MgCl_2$, 20 mM MES and cryoprotectant (BBY PS II).

Either 0.4 M sucrose or 30% v:v ethylene glycol was used as cryoprotectant.

PS II samples were stored at 10–18 mg/ml [chl] (typical oxygen evolving activity of 500–800 μmol O_2/mg chl/h) at 77K until used. Storage times were less than 15 weeks. No loss of ESR S_2 state photogeneratable signal intensity was observed over the storage period.

ESR samples were thawed on ice in darkness for 1 h before use. EDTA was added to the sample to reach a final concentration of 2 mM for Bricker PS II and 7 mM for BBY PS II. DCMU and artificial electron acceptors were omitted from all samples, as were monoalcohols to enable development of the $g = 4.1$ signals under all illumination regimes. Samples were transferred to quartz tubes and dark-adapted at room temperature for 10 min. Sample illumination was carried out in an N_2 gas flow cryostat, using a tungsten filament lamp filtered through 20 cm water, with strong yellow light at 130K (intensity ~ 600 W m^{-2}) and green light at 200K (light intensity ~ 300 W m^{-2}).

ESR studies were performed on two spectrometers; a Varian V-4502 X-band spectrometer and a Bruker ESP300E spectrometer, with an Oxford instruments ESR9 liquid helium cryostat operating between 4.5 and 40K, calibrated using either a carbon resistor or a gold-chromel thermocouple at the sample position. Data analysis was performed on an IBM compatible PC using home-written software or Bruker WIN EPR program.

For the temperature dependence studies, the unsaturated signal intensity was taken as the slope, extrapolated to zero microwave power (P), of a signal height vs $\sqrt{P}$ plot for the given signal (as described in Pace [17]). Signal heights were evaluated as previously described [17].

Exact, numerical solutions of field positions and transition intensities for model Hamiltonians were carried out using a public domain program (H.M. Gladney and J.D. Swalen, Quantum Chemistry Program Exchange, No. 134).

3. Results

The S_2 state signals generated from the different preparations containing the same cryoprotectant (e.g., Bricker PS II containing sucrose vs. BBY PS II containing sucrose) were essentially identical in line shape and temperature dependence behaviour, for the same illumination conditions. The differences in signal generation behaviours, i.e., multiline and $g = 4.1$ signal either cogenerated or individually generated, were due to the presence of the different cryoprotectants only. The results for each cryoprotectant and illumination temperature are presented as a combination of data from ESR experiments on PS II samples from each preparation type. All $g = 4.1$ signal spectra are presented as the illuminated minus the annealed (10 min at 290K) spectrum data.

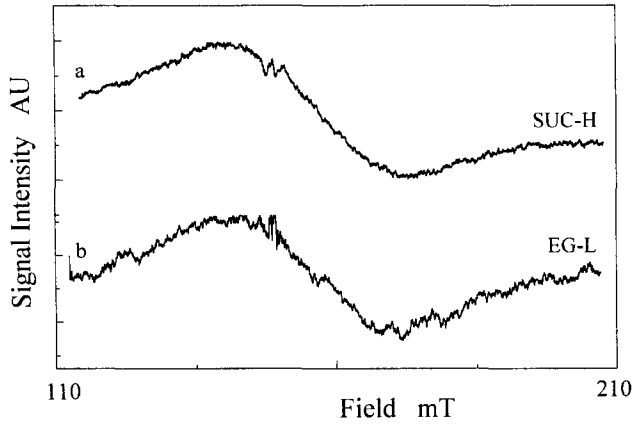

Fig. 1. Illuminated minus annealed spectrum of the $g = 4.1$ signal generated in (a) sucrose cryoprotected PS II illuminated at 200K (SUC-H-4.1), and (b) ethylene glycol cryoprotected PS II illuminated at 130K (EG-L-4.1). Spectrometer conditions: temperature 9K, microwave frequency 8.97 GHz, microwave power 11 mW, modulation frequency 100 KHz, modulation amplitude 1.7 mT.

Fig. 1a shows a $g = 4.1$ signal produced by illuminating sucrose cryoprotected PS II at 200K (termed SUC-H-4.1, see Abbreviations). The spectrum shows strong axiality, with a peak-to-trough width of 32 mT and g_{av} of 4.10 ± 0.02. No splitting of g ⊥ tensor components is resolved, nor is there any significant development of Mn hyperfine, such as that observed from PS II samples oriented onto mylar strips [29,30,34].

The temperature dependencies of the SUC-H-4.1 and cogenerated multiline have been shown to exhibit complementary deviations from Curie behaviour (Pace et al. [17]), with the multiline as ground state and $g = 4.1$ as first excited state. The simplest structure which could give rise to such behaviour [17] would be an antiferromagnetically exchange coupled Mn dimer differing in oxidation state by one. Total spin would be 7/2 for a MnIII-MnIV system, in which the multiline is the spin 1/2 ground and $g = 4.1$ the spin 3/2 first excited state. At sufficiently high temperature, such a system should exhibit a next excited spin 5/2 state at g ~ 6 (quasi axial as for the $g = 4.1$ signal). Fig. 2a shows a series of scans in the g8 ~ g3 region for SUC-H material over the temperature range 5K to 40K. It is apparent that intensity builds in the g ~ 6 region with increasing temperature. Moreover, this does not appear to be a line-broadening effect (see below). In addition, while signals at g ~ 6 can sometimes arise from partially denatured high spin cytochromes, these are not photogenerated at low temperature and normally subtract out in light minus dark difference spectra. In fact *no* g ~ 6 cytochrome signals are detectable in our uninhibited samples in illuminated or dark spectra.

The shape of the g ~ 6 signal may be estimated by

assuming it has negligible intensity in the 5K spectrum (i.e., 'pure' $g = 4.1$ spectrum), and subtracting appropriately scaled amounts of the latter from the higher temperature spectra. This assumes that the $g = 4.1$ signal shape does not change significantly with temperature, which appears to be the case, at least as far as its low field maximum position is concerned. Fig. 2b shows the shape of the g ~ 6 signal so obtained. We feel that this procedure reliably captures the form of the signal at the low field edge (around g ~ 6) but its shape at higher field is more uncertain. Interestingly, there may be a partially resolved hyperfine structure on this signal, with a mean minimum spacing of ~ 4 mT. Fig. 3 then shows the relative temperature dependencies of the multiline, $g = 4.1$ and g ~ 6 signals from the SUC-H material. The curves are theoretical fits to a dimer model which will be discussed below.

Fig. 1b shows the $g = 4.1$ generated by illuminating ethylene glycol cryoprotected PS II at 130K (termed EG-L-4.1). The overall shape of this signal is very similar to the SUC-H-4.1. The g_{av} for this signal is 4.11 ± 0.02, the peak-to-trough width is 28 mT, about 12% less than that for the SUC-H-4.1. No significant development of Mn hyperfine is apparent either on the $g = 4.1$ signal or in the $g = 2$ region (not shown); however, a slight splitting of the g ⊥ may be observed at the crossing point. This appears not to be due to a subtraction artefact from the rhombic

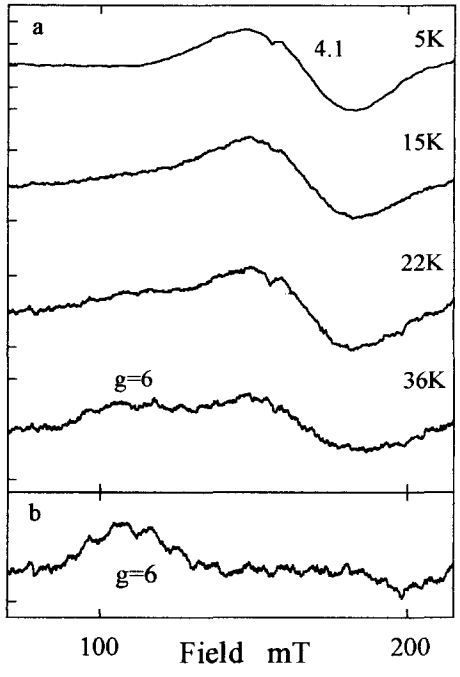

Fig. 2. (a) Temperature dependence of signal shapes in the g8 to g3 region for SUC-H material over the temperature range 5K to 40K. Spectrometer conditions: microwave frequency 9.423 GHz, microwave power 6.3 mW, modulation frequency 100 kHz, modulation amplitude 1.4 mT. All spectra are illuminated minus annealed. (b) Shape of g ~ 6 signal which builds at high temperature obtained by subtracting scaled amounts of the 5K or 9K spectrum from an average of the spectra obtained above 30K.

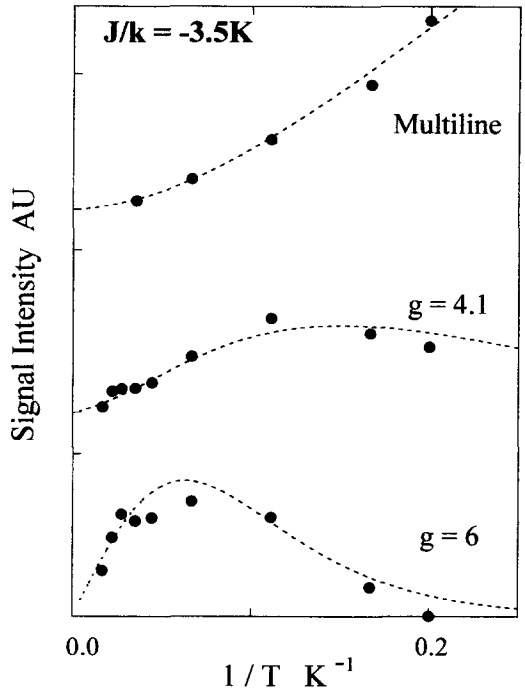

Fig. 3. Relative temperature dependences of the multiline, $g = 4.1$ and g ~ 6 signal intensities for SUC-H material. Intensities were obtained from signal amplitude versus √microwave power plots as previously described [17]. Signal amplitudes for the multiline and $g = 4.1$ signals were estimated as previously described [17], while that for the g ~ 6 signal was estimated by double integration in the g ~ 6 region of difference spectra as in Fig. 2b). Vertical scales are arbitrary due to different methods of signal quantitation. The curves are fits to a Mn III-IV dimer model as described in the text and Ref. [17].

iron ($g = 4.3$) signal, which occurs at lower field near the peak of this $g = 4.1$ signal. Overlap from the two components of the EG-L-4.1 signal hinders accurate evaluation of the apparent $g\perp_{1\&2}$ values. Fig. 4 shows the dependence of this $g = 4.1$ signal shape on temperature. In contrast to the case above with SUC-H material, little, if any, multiline signal is apparent, nor developed. The signal shape of the EG-L-4.1 is reasonably static between 8K and 16K. No obvious additional intensity develops in the g ~ 6 region with increasing temperature, nor any other region of this spectrum (covering g ~ 2.5 to g ~ 10). At the highest temperature, the EG-L signal appears to significantly broaden, unlike the SUC-H form. Fig. 5 shows the temperature dependence of the EG-L-4.1 signal amplitude. This exhibits clear, Curie-like isolated ground state behaviour over the range 5K to 40K. The curves are theoretical fits from a spin 5/2 state model discussed below.

While the two $g = 4.1$ signal types are superficially similar at X-band, the Q-band spectra (Fig. 6) reveal them to be distinct species, consistent with their qualitatively different temperature dependencies. The SUC-H-4.1 signal (Fig. 6a) now exhibits a resolved splitting of the apparent g ⊥ tensor components at the higher frequency. The g ⊥ components are estimated to be $g\perp_1 \approx 4.35 \pm 0.02$ and

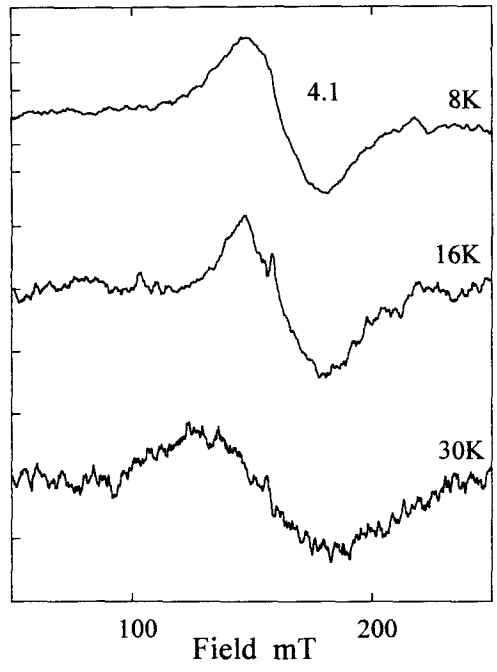

Fig. 4. Temperature dependence of signal lineshape in the g12 to g2.5 region for EG-L material over the temperature range 5K to 30K. Spectrometer conditions as in Fig. 2. All spectra are illuminated minus annealed.

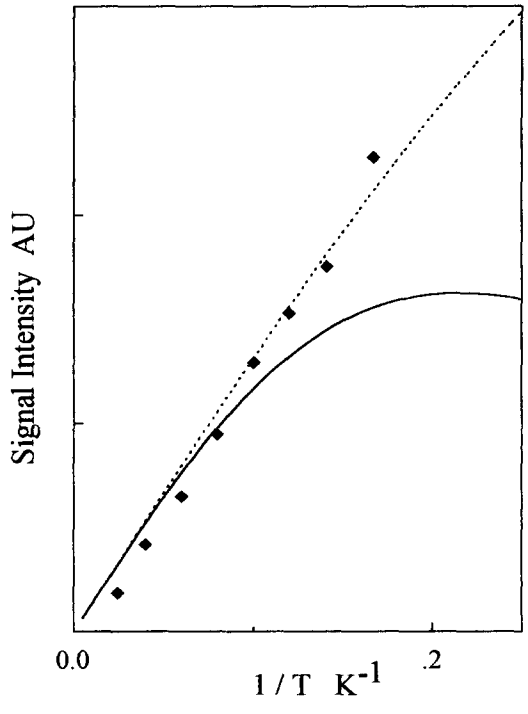

Fig. 5. Temperature dependence of the $g = 4.1$ signal intensity for the EG-L material. Intensities were obtained as in Fig. 3 and signal quanitation was by double integration around $g = 4$. The curves are fits to the Boltzmann model; Signal α $[\exp^{(-\Theta/T)}/(1 + \exp^{(-\Theta/T)} + \exp^{(-2\Theta/T)}]T^{-1}$ where $\Theta = 2.4$K (dotted curve) and $\Theta = 6.5$K (solid curve). See text and Ref. [17].

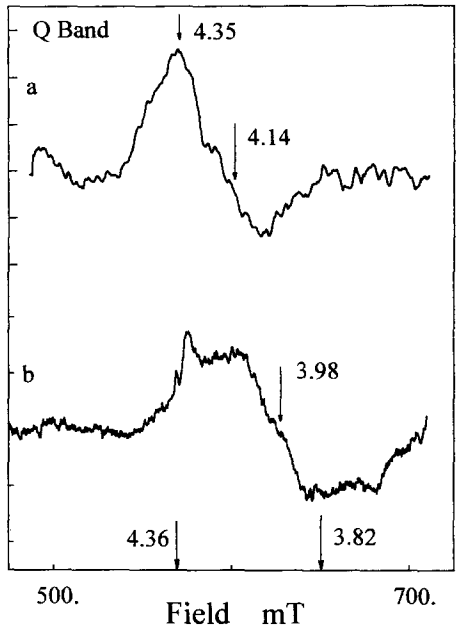

Fig. 6. Q band spectra for the SUC-H-4.1 (a) and the EG-L-4.1 (b) signals. These signals appear similar at X-band frequencies but become distinct at Q-band. Spectrometer conditions: temperature 9K, microwave frequency 34.75 GHz, microwave power 30 mW, modulation frequency 100 KHz, modulation amplitude 0.5 mT. The $g = 4.36$ and $g = 3.82$ positions refer to a rhombic spin 5/2 Hamiltonian discussed in the text.

$g\perp_2 \approx 4.14 \pm 0.02$ with $g_{av} \approx 4.25 \pm 0.02$. The peak-to-trough width of the signal is 47 mT. The SUC-H-4.1 signal shows strong axiality, similar to the X-band result, indicating a low E/D (≤ 0.02) [34]. The spectrum for the EG-L-4.1, Fig. 6b), is distinctively different to that of the SUC-H-4.1. While still apparently near axial, the g_{av} value for the EG-L-4.1 signal is $\approx 3.98 \pm 0.05$. The peak-to-trough width of this signal is 52 mT, and displays a very narrow crossing region. The wings of this spectrum are much broader than for the SUC-H-4.1.

Haddy et al. [22] have suggested that the $g = 4.1$ signal arises from the centre transition of a spin 5/2 state, which has near-rhombic anisotropy. For the uninhibited enzyme, they proposed a ZFS Hamiltonian with D = 0.43 cm^{-1} and E/D = 0.25. At frequencies below ~ 12 GHz, this system produces a strong quasi isotropic resonance in the g ~ 4 region, while above ~ 12 GHz, g ~ 4 resonances are observed only along two directions of the fine structure principle axes system (i.e., apparent $g_x \sim 0$). This Hamiltonian, with an effective gaussian line-width of ~ 35 mT, reproduced their experimental P-band (15 GHz) spectrum of the $g = 4.1$ signal quite well. The powder pattern simulation assumed an effective spin of 1/2, with an anisotropic g tensor, whose principle values were determined by exact solution of the ZFS Hamiltonian along the principle axis directions. Examination of the numerically computed (see Section 2) field positions and transition intensities for the above Hamiltonian at our Q-band frequency showed that strong turning points existed at g ~ 4.36 and g ~ 3.82, similar to the reported situation at

P-band [22]. However, numerous other turning point transitions of comparable intensity were predicted, from g ~ 12 to g ~ 3. Moreover, the angular dependence of the g ~ 3.82 transition was such that it would be the *high field* edge (i.e., the apparent g_x value) of an effective spin 1/2 system, with an apparent g_z value below ~ 8. The turning point at g ~ 3 is the low field edge of an unrelated group of transitions which extend down to g ~ 1.7. While a definitive conclusion must await an 'exact' numerical powder pattern simulation of the rhombic spin 5/2 Hamiltonian at Q-band, a non-trivial task, it is already clear that neither spectrum in Fig. 6 is consistent with turning points at *both* g ~ 4.36 *and* g ~ 3.82. More than anything, these spectra resemble the expected shapes for near axial spin 3/2 systems, which show no resolved g ⊥ splitting at X-band, but partial resolution of this splitting at Q-band.

4. Discussion

We observe two distinct '4.1' signals; one generated in sucrose cryoprotected PS II illuminated at 200K, which behaves as if arising from an excited state species, and another generated in ethylene glycol cryoprotected PS II illuminated at 130K, which behaves as if arising from a ground state species. Earlier [17], we showed that the temperature dependencies of the multiline and $g = 4.1$ signals from SUC-H material were consistent with them arising from the spin 1/2 and spin 3/2 states, respectively, of an antiferromagnetically coupled with Mn III-IV dimer. The coupling was weak, with $J/k \approx -3.0$K. The curves through the data points in Fig. 3 were generated by the same model, assuming now that the g ~ 6 signal arises from the next highest, spin 5/2, state in the manifold. Best overall fit was obtained with $J/k = -3.5$K, very similar to the earlier estimate. This now represents a far more stringent test of the dimer model, as a single parameter, J, specifies *all* three temperature dependencies, reflecting the multiplicities and energy levels of the three lowest states of the spin manifold. If the Mn cluster giving rise to the signals in Fig. 3 is not an isolated Mn III-IV dimer, then the evidence is compelling that it must be formally equivalent to such a system. This could arise, for instance, from a III-IV dimer weakly coupled to a strongly antiferromagnetic net spin zero pair (e.g., III-III or IV-IV). Either way, the $g = 4.1$ signal observed in SUC-H material is a near axial spin 3/2 centre, with ZFS parameters $D > 1$ cm^{-1} and $E/D \leq 0.02$, from the Q-band data.

Interpretation of the 'ground state', isolated g ~ 4 signal seen in 130K illuminated samples is less clear. This has been suggested to arise from the quasi-isotropic middle Kramer transitions of a rhombic spin 5/2 state, on the basis of modelling [22] (as discussed above) and recently, from a pulsed EPR study by Astashkin et al. [38]. This latter should, in principle at least, offer a direct determination of the spin state, based on the microwave field (H_1) intensity dependence of the echo amplitude in a two-pulse experiment. The analysis assumed that a quasi-isotropic effective g-value of ~ 4 would apply in calculating the microwave-induced transition probabilities for the presumed spin 5/2 state (weak field limit). We have found, however, from the exact numerical solution of the ZFS spin 5/2 Hamiltonian, using the parameters of Haddy et al. [22] required to simulate the X-band CW spectrum, that the transition probability is *not* isotropic for this system. It varies by a factor of ~ 2 depending on the H_1 and H_0 orientations in the molecular axis system, corresponding to an effective g-value range of 3.7 to 5.0. In essence, the 'weak field' approximation no longer applies in this system, with D comparable to the microwave quantum. This has significant implications for the interpretation of the echo H_1 dependence, as is apparent from the actual data presented by Astashkin et al. Their dark-annealed sample (Fig. 4, Ref. [38]) has a substantial contribution in the g ~ 4 region from the rhombic iron g ~ 4.3 signal, as expected. This signal is a 'gold standard' rhombic centre doublet, spin 5/2 state, with (conventional nomenclature) D ~ 0.4 cm^{-1} and E/D ~ 0.3 [17,39], parameters very similar to those invoked for the Mn $g = 4.1$ signal. However, the echo magnitude versus H_1 dependence at $g = 4.1$ for this annealed sample (Fig. 5a, Ref. [38]), as reported by the authors, shows *no* peak at g ~ 4, as would be expected from their analysis, but rather, a broad distributed response in the g ~ 5 to g ~ 2 region. Even allowing for cavity background contributions, alluded to by the authors, this is a surprising result. It is, however, qualitatively what one would expect at X-band for a species with the above ZFS parameters and raises serious doubts concerning the assignment of the g ~ 4.1 signal by Astashkin et al. [38].

The simple shapes of the two $g = 4.1$ signal types seen at Q-band (Fig. 6) suggest that if these were to arise from spin 5/2 states, then D should be large enough that all three turning points are visible in the g ~ 4 region at this frequency. This requires $D \geq 1.2$ cm^{-1}, a circumstance which would also make the assumption of an isotropic transition probability at X-band more reasonable. However, the centre doublet from which the g ~ 4 signal arises is an excited state. If D = 0.43 cm^{-1} and E/D ~ 0.3 (as in Ref. [22]), then this state is separated by ± 1.5 cm^{-1} from the ground and top states. The dotted curve in Fig. 5 is the best fit to the X-band intensity data of a Boltzmann model assuming this value of the spacing. Although it clearly goes against the trend of the data, it could not be excluded because the curvature is modest over the temperature range studied. However, if D is ~ 1.2 cm^{-1}, the state spacing is over 4 cm^{-1}. A Boltzmann model with this spacing is excluded by the data (solid curve in Fig. 5). Thus, a rhombic spin 5/2 model of the isolated $g = 4.1$ signal with low D (~ 0.4 cm^{-1}) is allowed by the X-band signal temperature dependence, but argued against by the Q-band and (ironically) the spin echo data. A similar model with D large enough to accommodate the Q-band spectral data is

excluded by the temperature dependence of the signal at X-band. We are left with the conclusion that any identification of the signal as a spin 5/2 state is difficult to rationalise with all the data now available.

The most obvious interpretation we can place on the EG-L-4.1 signal, from our data, is that it arises from a near axial spin 3/2 ground state. D would be less (< 1 cm^{-1}) than for the case of the SUC-H-4.1 excited state signal, as there is now a detectable drop in the central g ⊥ value (4.10 to 3.98) going from X to Q-band (Fig. 6). To be consistent with the spin echo results and the fact that the resonance is centred above $g = 4.0$ at low frequencies (S-, X-bands), the true g ⊥ of the state would have to be above 2 (2.1–2.2). This would also apply to the SUC-H-4.1 signal form. In fact, precisely this effect is observed in the spin 3/2 states of model compounds containing weakly coupled Mn dimers [40,41]. The origin of the effect has been discussed elsewhere [34].

It is well known, and confirmed by us, that the $g = 4.1$ signal formed by 130K illumination interconverts to the multiline signal on brief annealing of the sample at 200K. As noted earlier, this observation was originally interpreted by Casey and Sauer [13] to mean that the $g = 4.1$ signal arose from an electron transfer intermediate between the Mn multiline centre and the Z^+/P680 centres. We favour this view, especially in light of the fact that the multiline signal at S, X- and Q-bands may be successfully simulated using an isolated dimer model with unusual, anisotropic Mn nuclear hyperfine and quadrupolar couplings [24].

A plausible conclusion from all the above and our earlier results [17,24,34], is that the 4 Mn are organised as two coupled pairs, which are magnetically isolated from each other, but close enough for rapid electron transfer (Fig. 7). One pair is responsible for the multiline and excited state $g = 4.1$ and g ~ 6 signals. The antiferromagnetic exchange coupling in this pair may be modulated by buffer effects: in the absence of low molecular weight mono alcohols (< 3% MeOH, EthOH), it is only a few cm^{-1}. In the presence of alcohols, it is at least tens of cm^{-1}, resulting in a multiline only signal being observed at temperatures below ~ 30K, with essentially Curie behaviour [17]. This pair we would also associate with the S-state turnover, at least for the S_1 to S_2 state transition. So the S_1 state parallel polarisation EPR signal observed by Dexheimer et al. [42] should arise from this Mn III-III pair, in its first excited (spin = 1) state.

The second pair, to which we ascribe an electron transfer/charge accumulation role, would be functionally (and presumably spatially) closer to Z/P680. Since an isolated Mn pair with conventional oxidation levels would not yield a spin 3/2 ground state, at least one additional spin centre must be involved. The most obvious candidate is an oxidisable protein side chain which is a ligand to the system. Histidine or tyrosine are possibilities [43,44], although the presence of radicals arising from these residues have been reported so far only in Ca^{2+} depleted systems,

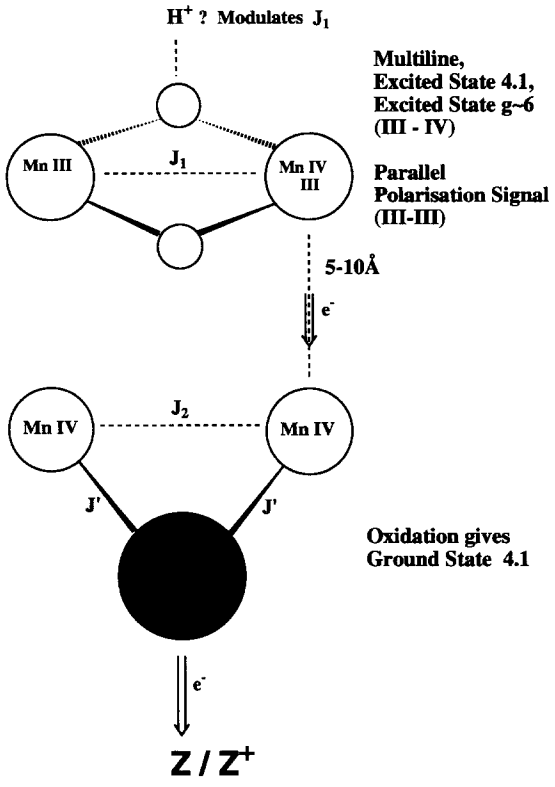

Fig. 7. Possible model for the two Mn dimer structures within the OEC. The magnetic interactions giving rise to each type of formal S_2 state signal are illustrated. For the behaviours described in the text, the dimers must be magnetically isolated from each other but within rapid electron transfer range (5Å to 10Å). The $S = 1/2$ species in the lower dimer, generating the ground state $g = 4.1$ signal, is probably an oxidisable amino acid side chain. Its location as a bridging ligand is speculative, but readily accomodates a spin 3/2 ground state (see text and Ref. [27]). The parallel polarisation signal of Dexheimer et al. [42] is presumed to arise from the upper dimer when in the Mn III-III state. This state can coexist with the ground state form of the $g = 4.1$ signal, but not with the multiline or excited state form of the $g = 4.1$ signal. The lower dimer may be a charge transfer/redox equivalent accumulator and the water oxidation chemistry may then occur at only one dimer, presumably that responsible for the multiline signal. Buffer effects, possibly influencing the μ-oxo bridge protonation state, are presumed to modulate the magnitude of antiferromagnetic exchange coupling in this pair.

and their relevance to the model in Fig. 7 is as yet unclear. If the oxidisable side chain is a bridging ligand (spin 1/2), equally ferromagnetically coupled to the two equal spin, antiferromagnetically coupled Mn ions of this centre, the resulting system may have a spin 1/2, 3/2 or 5/2 ground state. The actual value depends on a balance of the exchange couplings [27].

The model in Fig. 7 would provide a natural explanation for the results of Dexheimer et al. [42], who observed that the S_1 state parallel polarisation signal was lost only on the formation of the multiline, but not the (ground state) $g = 4.1$ signal. Although the multiline and ground $g = 4.1$ signals are both 'formal S_2 state' signals in our picture, they arise from unconnected centres. This interpretation of the Mn organisation in PS-II is also totally consistent with

the strong conclusion from EXAFS, namely that each Mn has one Mn neighbour at ~2.7 to 2.8Å [6–9,45,46]. It would require, however, that the 3.3 to 3.6Å Mn-metal peak be a Mn-Ca rather than Mn-Mn distance. At present, the reported uncertainty in the assignment of the 3.3Å peak would appear to admit this possibility.

Acknowledgements

The authors would like to thank Drs D. MacLachlan, T. Wydrzynski and J. Anderson for useful discussions during experimentation and preparation of the manuscript. Especially, we wish to thank Dr R. Bramley for use of the Q-band spectrometer and assistance with the numerical simulations. This work was supported through the Australian Research Council. P.J.S. was supported by a Plant Science CRC Postgraduate Student Support Scholarship.

References

[1] Yocum, C.F., Yerkes, C.T., Blankenship, R.E., Sharp, R.R. and Babcock, G.T. (1981) Proc. Natl. Acad. Sci USA 78, 12, 7507–7511.
[2] Debus, R.J. (1992) Biochim. Biophys. Acta 1102, 269–352.
[3] Rutherford, A.W., Boussac, A. and Zimmermann, J.-L. (1991) New J. Chem. 15, 491–500.
[4] Renger, G. and Wydrzynski, T. (1991) Biol. Metals 4, 73–80.
[5] Kok, B., Forbush, B. and McGloin, M. (1970) Photochem. Photobiol. 11, 457–475.
[6] Cole, J.L., Yachandra, V.K., McDermott, A.E., Guiles, R.D., Britt, R.D., Dexheimer, S.L., Sauer, K. and Klein, M.P. (1987) Biochemistry 26, 5967–5973.
[7] Yachandra, V.K., Guiles, R.D., McDermott, A.E., Cole, J.L., Britt, R.D., Dexheimer, S.L., Sauer, K. and Klein, M.P. (1987) Biochemistry 26, 5974–5981.
[8] MacLachlan, D.J., Hallahan, B.J., Ruffle, S.V., Nugent, J.H.A., Evans, M.C.W., Strange, R.W. and Hasnain, S.S. (1992) Biochem. J. 285, 569–576.
[9] Yachandra, V.K., deRose, V.J., Latimer, M.J., Mukerji, I., Sauer, K. and Klein, M.K. (1993) Science 260, 675–679.
[10] Dismukes, G.C. and Siderer, Y. (1981) Proc. Natl. Acad. Sci. USA 78, 274–278.
[11] Hansson, Ö. and Andréasson, L.-E. (1982) Biochim. Biophys. Acta 679, 261–268.
[12] Brudvig, G.W., Casey, J.L. and Sauer, K. (1983) Biochim. Biophys. Acta 723, 366–371.
[13] Casey, J.L. and Sauer, K. (1984) Biochim. Biophys. Acta 767, 21–28.
[14] Zimmermann, J.-L. and Rutherford, A.W. (1984) Biochim. Biophys. Acta 767, 160–167.
[15] De Paula, J.C., Innes, J.B. and Brudvig, G.W. (1985) Biochemistry 24, 8114–8120.
[16] Zimmermann, J.-L. and Rutherford, A.W. (1986) Biochemistry 25, 4609–4615.
[17] Pace, R.J., Smith, P.J., Bramley, R. and Stehlik, D. (1991) Biochim. Biophys. Acta 1058, 161–170.
[18] Dismukes, G.C., Ferris, K. and Watnick, P. (1982) Photobiochem. Photobiophys. 3, 243–256.
[19] Andréasson, L.-E., Hansson, Ö. and Vängård, T. (1983) Chem. Scripta 21, 71–74.
[20] Haddy, A., Aasa, R. and Andréasson, L.-E. (1989) Biochemistry 28, 6954–6959.
[21] Vängård, T., Hansson, Ö. and Haddy, A. (1990) in Manganese Redox Enzymes (Pecoraro, V. L. ed), pp. 105–118, VCH, NY.
[22] Haddy, A., Dunham, W.R., Sands, R.H. and Aasa, R. (1992) Biochim. Biophys. Acta 1099, 25–34.
[23] Kusonoki, M. (1992) Chem. Phys. Lett. 197, 108–116.
[24] Åhrling, K.A. and Pace, R.J. (1995) Biophys. J. 68, 2081–2090.
[25] Hansson, Ö., Andrëasson, L.-E. and Vängård, T. (1984) in Advances in Photosynthesis Research (Sybesma C. ed), Vol. 1, pp. 307–310, Martinus Nijhoff/Dr. W. Junk, The Hague.
[26] Britt, R.D., Lorigan, G.A., Sauer, K., Klein, M.P. and Zimmermann, J.-L. (1992) Biochim. Biophys. Acta 1040, 95–101.
[27] de Paula, J.C., Beck, W.F. and Brudvig, G.W. (1986) J. Am. Chem. Soc. 108, 4002–4009.
[28] Kougliotis, D., Hirsch, D. and Brudvig, G.W. (1992) J. Am. Chem. Soc. 114, 8322–8323.
[29] Kim, D.H., Britt, R.D., Klein, M.P. and Sauer, K. (1990) J. Am. Chem. Soc. 112, 9389–9392.
[30] Kim, D.H., Britt, R.D., Klein, M.K. and Sauer, K. (1992) Biochemistry 31, 541–547.
[31] Klein, M.P., Sauer, K. and Yachandra, V.K. (1993) Photosynth. Res. 38, 265–277.
[32] Cole, J., Yachandra, V.K., Guiles, R.D., McDermott, A.E., Britt, R.D., Dexheimer, S.L., Sauer, K. and Klein, M.P. (1987) Biochim. Biophys. Acta 890, 395–398.
[33] Hansson, Ö., Aasa, R. and Vängård, T. (1987) Biophys. J. 51, 825–832.
[34] Smith, P.J., Åhrling, K.A. and Pace, R.J. (1993) J. Chem. Soc. Faraday Trans. 89, 2863–2868.
[35] Bricker, T.M., Pakrasi, H.B. and Sherman, L.A. (1985) Arch. Biochem. Biophys. 237, 170–176.
[36] Berthold, D.A., Babcock, G.T. and Yocum, C.F. (1981) FEBS Lett. 134, 231–234.
[37] Beck, W.F., De Paula, J.C. and Brudvig, G.W. (1985) Biochemistry 24, 3035–3043.
[38] Astashkin, A.V., Kodera, Y. and Kawamori, A. (1994) J. Magn. Res. Ser. B 105, 113–119.
[39] Castner, T. Jr., Newell, G.S., Holton, W.C. and Slichter, C.P. (1960) J. Chem. Phys. 32, 668–673.
[40] Chang, H.-R., Larsen, S.K., Boyd, P.D.W., Pierpont, C.G. and Hendrickson, D.N. (1988) J. Am. Chem. Soc. 110, 4565–4576.
[41] Larson, E., Haddy, A., Kirk, M.L., Sands, R.H., Hatfield, W.E. and Pecoraro, V.L. (1992) J. Am. Chem. Soc. 114, 6263–6265.
[42] Dexheimer, S.L. and Klein, M.P. (1992) J. Am. Chem. Soc. 114, 2821–2826.
[43] Boussac, A., Zimmermann, J.-L., Rutherford, A.W. and Lavergne, J. (1990) Nature 347, 303–306.
[44] Hallahan, B.J., Nugent, J.H.A., Warden, J.T. and Evans, M.C.W. (1992) Biochemistry 31, 4562–4573.
[45] Larson, E.J., Riggs, P.J., Penner-Hahn, J.E. and Pecoraro, V.L. (1992) J. Chem. Soc. Chem. Commun. 39, 102–103.
[46] George, G.N., Prince, R.C. and Cramer, S.P. (1989) Science 243, 789–791.